

In presenting the dissertation as a partial fulfillment of the requirements for an advanced degree from the Georgia Institute of Technology, I agree that the Library of the Institute shall make it available for inspection and circulation in accordance with its regulations governing materials of this type. I agree that permission to copy from, or to publish from, this dissertation may be granted by the professor under whose direction it was written, or, in his absence, by the Dean of the Graduate Division when such copying or publication is solely for scholarly purposes and does not involve potential financial gain. It is understood that any copying from, or publication of, this dissertation which involves potential financial gain will not be allowed without written permission.

3/17/65

b

LATERAL PRESSURES AGAINST A PILE
IN A COHESIONLESS SOIL

A THESIS

Presented to
The Faculty of the Graduate Division

by

F. David Shiver

In Partial Fulfillment
of the Requirements for the Degree
Master of Science in Civil Engineering

Georgia Institute of Technology

April, 1967

LATERAL PRESSURES AGAINST A PILE
IN A COHESIONLESS SOIL

Approved: _____

Chairman _____

Date approved by Chairman: 5/10/07

ACKNOWLEDGMENTS

The author wishes to express his appreciation to Professor George F. Sowers for his suggestions and help throughout this project.

To Professors Billy B. Mazanti and Neil H. Wade, thanks are offered for their sincere interest and help throughout the project.

To my wife, Janet, I wish to express deep gratitude for her untiring patience and assistances which helped make this work possible.

TABLE OF CONTENTS

	Page
ACKNOWLEDGMENTS.	ii
LIST OF TABLES	iv
LIST OF ILLUSTRATIONS.	v
SUMMARY.	vi
Chapter	
I. INTRODUCTION.	1
II. THEORY.	3
III. TEST APPARATUS AND MATERIAL	12
IV. TEST PROCEDURE.	22
V. DISCUSSION OF RESULTS	32
File Depth of 10 Feet	
File Depth of 15 Feet	
VI. CONCLUSIONS	41
VII. RECOMMENDATIONS	42
BIBLIOGRAPHY	43

LIST OF TABLES

Table		Page
1.	Lateral Pressure Coefficients for Piles.	11
2.	Maximum and Minimum Densities.	19
3.	Shear Strength Characteristic.	19
4.	Penetrometer Test Results.	33
5.	K versus Pressure and Depth.	36
6.	K versus Pressure and Depth.	38

LIST OF ILLUSTRATIONS

Figure		Page
1.	Theoretical Bearing Capacity Factors	7
2.	Terzaghi Relationship Between Wall Movement and Horizontal Earth Pressure.	9
3.	Pile Shaft Dimensions.	13
4.	Wiring Diagram for Lateral Load Cells.	15
5.	Lateral Pressure Load Cell	16
6.	Base Plate Load Cell	18
7.	Penetrometer Proving Ring Calibration.	21
8.	Gauge 1 -- Lateral Load Cell Calibration	24
9.	Gauge 2 -- Lateral Load Cell Calibration	25
10.	Gauge 3 -- Lateral Load Cell Calibration	26
11.	Gauge 4 -- Lateral Load Cell Calibration	27
12.	Base Plate Proving Ring Calibration.	28
13.	Relationship Between Depth and Total Penetration Resistance for Different Sand Densities.	31
14.	Area Pressure Curves at 10 Feet.	37
15.	Area Pressure Curves at 15 Feet.	39

SUMMARY

The purpose of this investigation was to determine the effects of lateral and vertical pressures on the ultimate bearing capacity of a pile in a cohesionless soil.

A pile, 15 feet long and 4-1/2 inches in diameter was driven into an eight foot diameter pit filled with sand of uniform density. The pile was instrumented with load cells at four different depths to measure the lateral pressures against its sides. A proving ring at the tip of the pile provided a method for determining the vertical force on the embedded end of the pile.

Readings were taken from all the gauges before and after driving. The difference between these readings indicated the lateral load of the sand against the pile. After the readings had been taken, the pile was loaded to failure by jacking down on the top of the pile with an hydraulic ram which reacted against a steel loading frame. The maximum load was determined from the pressure in the jack, and the vertical load against the tip of the pile was read from the proving ring. The load determined from the proving ring was subtracted from the maximum load read from the jack and was attributed to side load.

The anticipated end load was calculated using the general bearing capacity equation with Meyerhof's constants and was found to be approximately 20 percent larger than the actual end load measured. This indicated Meyerhof's factors to be on the unsafe side for the soil used.

The actual lateral pressures were used to calculate average values of K , the ratio of the overburden pressure to the lateral pressure, for the different gauge depths. Values of K varied from a maximum at the top of the pile to a minimum at its tip. The deeper the pile was driven, the smaller the average value of K obtained. The lateral force at the embedded end decreased slightly as the pile was pushed into the sand.

The average value of K necessary to obtain the measured skin friction load was calculated using a linear pressure distribution curve. This value was approximately equal to one in each case. The area under the triangular distribution curve was approximately equal to the area under the actual pressure distribution curve, indicating that the use of a linear pressure distribution curve was a good approximation for determining the ultimate bearing capacity of a pile of the approximate lengths used in this study.

CHAPTER I

INTRODUCTION

With the larger and heavier structures being built in modern times, foundations have become a more critical problem. Because the surface soil is often incapable of carrying the design loads for heavier structures, it may become necessary to use deep foundations.

Many of the deep foundations used today are piles; however, the knowledge of the behavior of pile foundations has not kept up with their increase in use. This has led to both over design and under design where men and money were lost. Because of the lack of information, there is an ever growing need for research into pile designs and failures.

The load carrying capacity of a pile is the sum of the end bearing and the skin friction. The skin friction resistance is the sum of the vertical resistant forces acting along the side of the pile. The end bearing is the vertical resistance offered at the tip of the pile. Most piles develop their ultimate load carrying capacity from a combination of both skin friction and end bearing. The material in which the pile is placed, together with the depth of penetration, will determine which of the two components contribute the larger resistance.

The ultimate load carrying capacity of a pile driven into a cohesionless material is comprised of both skin friction and end bearing. It is recognized that these components are dependent on many variables, such as the roughness and shape of the pile surface, the taper of the

pile, and the volume of soil displaced. The end bearing of a pile has been the subject of study by many investigators, among these being Hansen (1), Terzaghi (2), Caquot (3), Skempton (4), and Meyerhof (5). The results of most of these studies can be expressed by the general bearing capacity equation. Researchers have used different bearing capacity coefficients for the same soil conditions indicating disagreement in determining the coefficients.

The skin friction resistance in a cohesionless soil is proportional to the lateral pressures against the sides of the pile. Problems arise here, for little information is available about this lateral pressure. The pressure is usually assumed to be intermediate between the at-rest earth pressure and the passive earth pressure.

The purpose of this research was to obtain a better understanding of the load carrying capacity of a pile by determining the end bearing resistance and total lateral pressure skin friction resistance against the pile. Strain gauges placed on the embedded pile were used to determine the magnitude of the vertical force on its tip and the lateral pressures on its sides during failure. The cohesionless soil into which the pile was driven was placed in a uniform manner to achieve constant density throughout. Load cells containing strain gauges were placed at various depths along the pile to measure the lateral pressures, and a proving ring was placed in the embedded end of the pile to measure the vertical pressure at the tip.

CHAPTER II

THEORY

The load carrying capacity of a pile is composed of skin friction and end bearing. The end bearing is the force against the tip of the pile and can be calculated by considering the tip of the pile to be a footing below the soil surface. According to Terzaghi (6), this can be expressed by

$$q_o = \frac{\gamma b}{2} N_\gamma + q' N_q + C N_C \quad (1)$$

where q_o denotes the end bearing of the pile

γ denotes the unit weight of the soil

b is equal to 0.9 times the diameter of the pile

C denotes soil cohesion

q' denotes surcharge

N_γ shows influence of soil weight and foundation width

N_C shows influence of cohesion

N_q shows influence of surcharge

For a cohesionless soil, the cohesion, C , is zero, and the equation can be rewritten as

$$q_o = \frac{\gamma b}{2} N_\gamma + q' N_q \quad (2)$$

Since b is small, the equation can be expressed by

$$q_o = q' N_q \quad (3)$$

The skin friction depends on the forces acting along the side of the pile and on the roughness and shape of the surface of the pile. This may be expressed by

$$Q_F = S \cdot A \quad (4)$$

where S = the unit resistance along the side of the pile

A = the surface area of the pile

The area of the pile is

$$A = \int_0^H \pi D dz \quad (5)$$

where D = the diameter of the pile

H = the depth of the pile

and the unit skin resistance, S , can be expressed by

$$S = a + \bar{p} \tan \delta \quad (6)$$

where a = adhesion

\bar{p} = effective lateral pressure against the pile

δ = angle of sliding or skin friction

In a cohesionless soil, there is no adhesion between the soil and

the sides of the pile. Therefore, the unit skin resistance becomes

$$S = \bar{p} \tan \delta \quad (7)$$

The average effective pressure, \bar{p} , is generally assumed to be proportional to the overburden pressure and if so can be expressed by

$$\bar{p} = K \bar{q} \quad (8)$$

where K is a dimensionless coefficient of lateral earth pressure

\bar{q} is the vertical overburden pressure at a given depth

The average overburden pressure, \bar{q} , may be expressed by

$$\bar{q} = \gamma z - u \quad (9)$$

where z is the depth below the soil surface along the pile

u is neutral pressure

Combining terms, the total skin resistance becomes

$$Q_F = \int_0^H \pi DK (\gamma z - u) \tan \delta \cdot dz \quad (10)$$

The ultimate bearing capacity of a pile in a cohesionless soil can be expressed by

$$Q_u = q_o A + Q_F \quad (11)$$

substituting

$$Q_u = \left(\frac{\gamma b}{2} N_\gamma + q' N_q \right) A + \int_0^H K \pi D (\gamma z - u) \tan \delta \, dz \quad (12)$$

N_q and N_γ values have been determined by many investigators. Comparisons of these values show a significant lack of agreement, as depicted in Figure 1.

Norlund (7) worked with actual piles in the field and determined that the average side resistance of a pile was a function of the friction angle of soil, the angle of friction between the soil and the pile, the taper of the pile, the minimum perimeter encompassing the pile, and the volume of displaced soil per unit length of the pile. Norlund's equation for side resistance can be expressed by

$$P_S = \sum_{d=0}^{d=D} K_0 P_d \tan \delta C_d \Delta_d \quad (13)$$

where P_S = the side resistance in psi

d = depth from ground surface to the point of the pile

K_0 = a dimensionless factor expressing the ratio of the resultant of the effective normal and shear stresses on an incipient failure plane passing through a point and the effective overburden pressure at that point

P_d = effective overburden pressure

δ = friction angle on surface of sliding

C_d = minimum pile perimeter

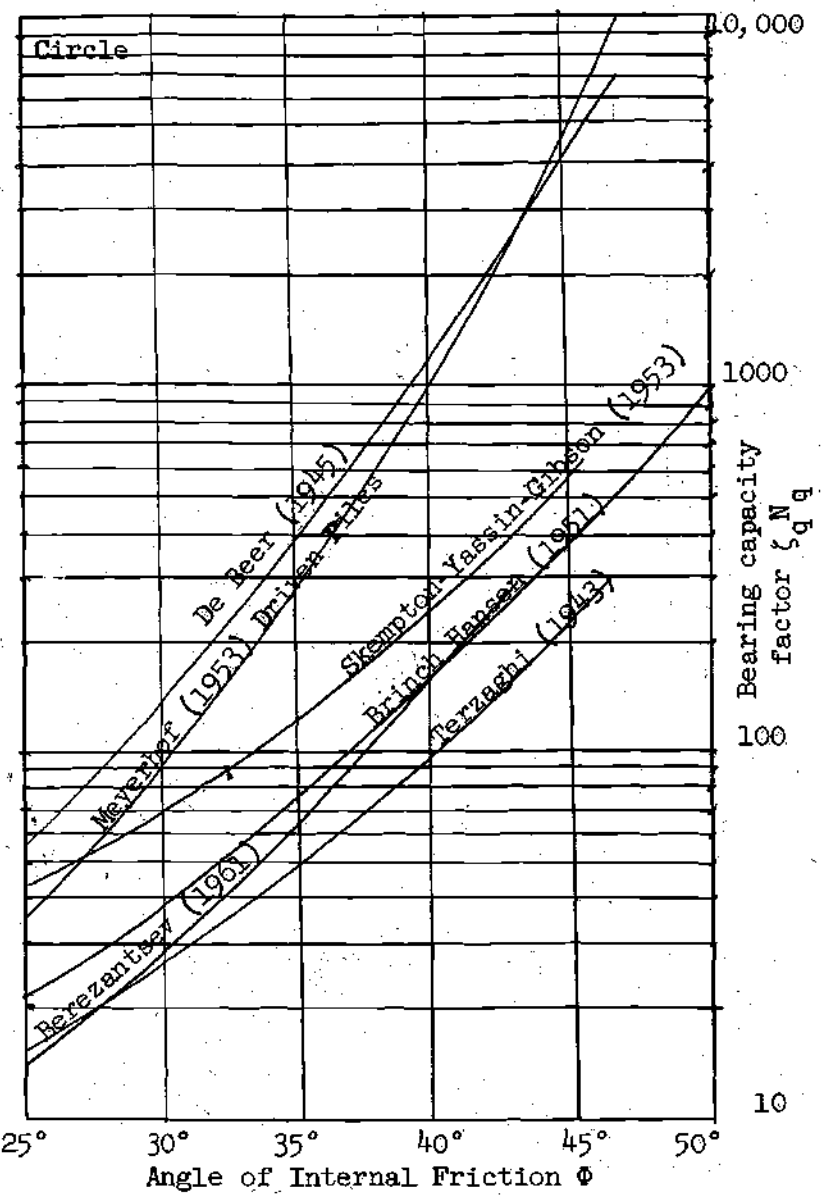
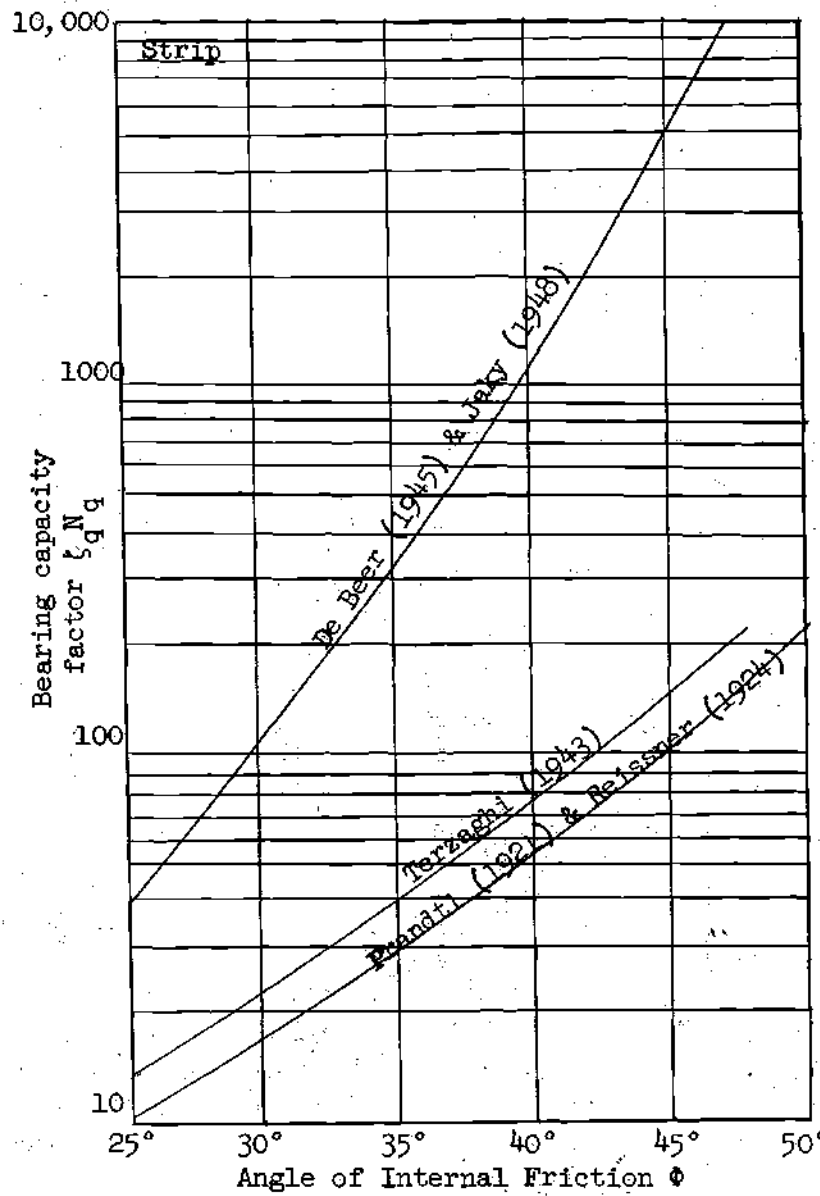
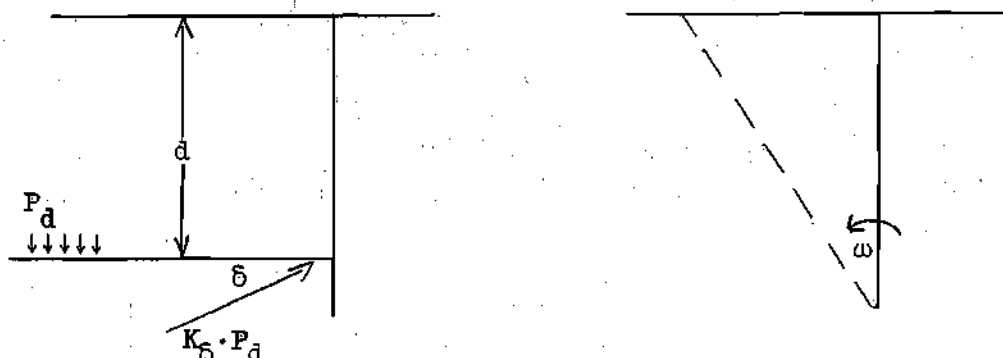


Figure 1. Theoretical Bearing Capacity Factors

To determine values for K_0 , Norlund considered the hypothetical case of an infinitely long, nondisplacement wall, which is allowed to rotate an angle of ω as shown below.



When ω is zero, K_0 is equal to K_0 and has the value of $0.5 \sec \delta$, this being the lower limit. As ω increases, the pressure on the side of the wall increases until a critical value is reached beyond which further increase in ω will not increase K_0 . This maximum pressure is the ultimate "passive" pressure.

A. Caquot and J. Kerisel (8) determined values for K_0 at the ultimate limit for a cohesionless soil by considering the stability of a failure wedge whose surface of failure was a combined curve and plane. Their solution is valid when $\delta = \phi$.

Terzaghi (9) investigated the relationship between earth pressure and the yielding of a retaining wall. He found there was almost no difference in earth pressures when the wall was allowed to rotate and when the wall was allowed to move laterally. Using the information he discovered, Terzaghi found a relationship between K_0 and ω , δ , as is illustrated in Figure 2. Norlund has tried to relate Terzaghi's findings to

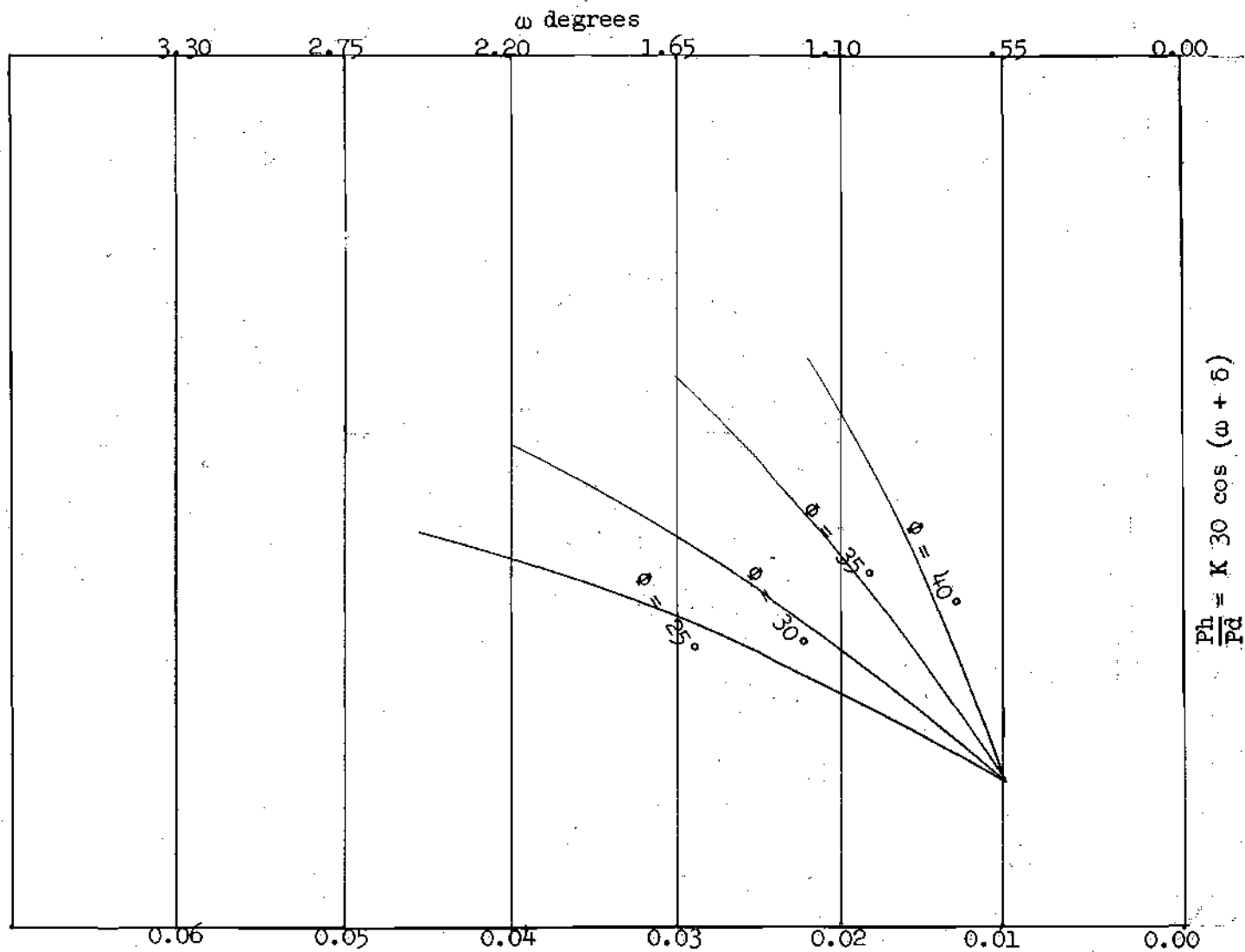


Figure 2. Terzaghi Relationship Between Wall Movement and Horizontal Earth Pressure

piles.

Norlund's method of determining the ultimate bearing capacity of a pile assumed that the skin-friction resistance and end-bearing capacity could be evaluated independently. Broms (10) stated that model tests by A. Kezdi (11) have indicated that the end-bearing capacity of a pile is affected by the skin-friction resistance. This effect has been attributed to an increase in effective overburden pressure by the load carried through skin-friction.

Model tests conducted at Cornell University by J. O. Silberman (12) indicated that K is affected by the degree of pile taper, loading conditions, and relative density of the soil surrounding the pile. A white uniform quartz sand was used in Silberman's work, and the maximum and minimum densities were determined. The skin-friction resistance of the piles was determined with respect to pull-out (tension), axial load, and rotation (torsion). For the tension tests, the average K values were 0.22 and 4.65 at low and at high relative densities of the sand, respectively. The results of the torsion tests were 0.03 and 2.95, and the results of the compression tests were 0.60 and 9.84. In the compression tests, the coefficient of lateral earth pressure was increased many times over, possibly as the result of an increase in relative density. This represented an increase in friction angle from 28.0 degrees to 33.0 degrees.

The Cornell test indicated that K was highly sensitive to the method of loading and the relative density of the soil. Norlund's method assumed that K was independent of the relative density. Norlund's method should be on the safe side provided that the shear strength parameter of the soil can be estimated correctly.

Broms stated further that the large effect of relative density on the skin-friction resistance can be attributed to arching. As the pile is loaded, the load is transferred into the surrounding soil causing a volume change. At high relative densities, the volume changes are resisted by an increase of lateral pressure because the compressibility of dense sand is small. At low relative densities, the volume decreases and the lateral pressure decreases.

Sowers and Sowers (13) state that K is a variable depending on how the pile was placed in the soil and on the initial relative density of the sand. Table 1 shows their values.

Table 1. Lateral Pressure Coefficients for Piles

Condition	K
Bored or jettted pile	0.5
Pile jettted, then driven few feet	1
Pile driven in loose soil	1
Pile driven in dense soil	2-4

CHAPTER III

TEST APPARATUS AND MATERIAL

This investigation was undertaken to get a better understanding of the bearing capacity of a pile. Tests consisting of the driving and loading of a specially constructed pile were performed. The pile was made to withstand the force of driving into a cohesionless material and to measure both lateral and vertical pressures against it before and after loading.

To withstand the force of driving the 15 foot pile into the sand, the pile shaft was made of a 4-1/2 inch outside diameter steel pipe with a wall thickness of 3/4 inch. The pile is shown in Figure 3. Since it was desirable to measure the lateral load on the pile at different depths below the ground surface, the pile was made in sections with a lateral pressure measuring device between each section. There were four sections, three 4 foot sections and one 1-1/2 foot section. The short section was placed at the bottom so as to have as many load cells near the foot of the pile as possible.

To measure the lateral pressure, a special load cell was constructed. This instrument was required to withstand the shock of driving and the shearing forces that were applied to it during driving, and it was to be sufficiently sensitive to measure the relatively small magnitudes of lateral earth pressure against it. Furthermore, these instruments acted as connections between the different pile sections. Since

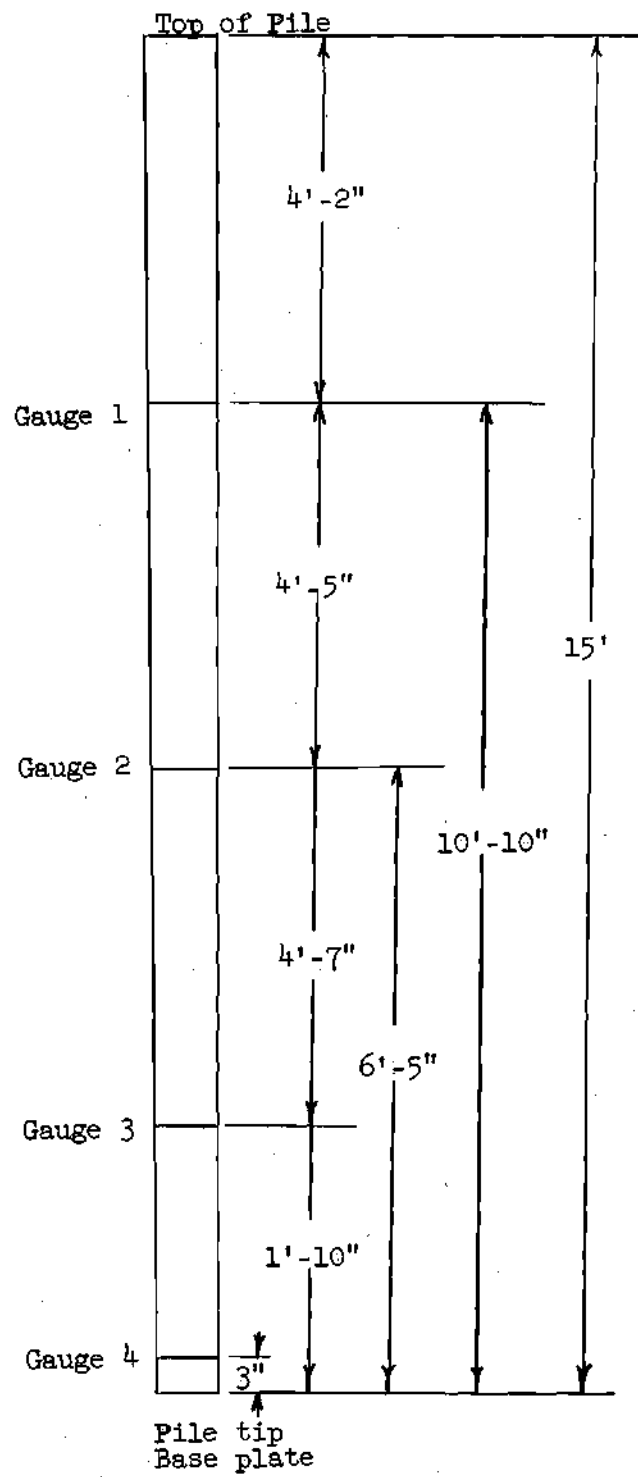


Figure 3. Pile Shaft Dimensions

the pile was driven, loaded and subsequently pulled, it was necessary for these connections to withstand both compressive and tensile forces.

Four and one-half inch diameter solid steel cylinders were selected for the connections. Four cylinders were machined to 5-1/4 inches in length and a 1-1/2 inch diameter hole was drilled in the center of each. Slots one inch long by 3/4 inch deep were cut on the outside of both ends of the cylinders so that the pile shaft would fit tightly over the end of each connection and could be bolted to it.

Tubular aluminum pressure cells were used to measure the small lateral pressures. The pipe was 4-1/2 inches in outside diameter and was cut in sections 1-1/4 inches long. The inside of the aluminum rings was machined to approximately 0.01 inch in thickness to increase flexibility. Four SR-4 type AP-12 strain gauges were placed around the inside of each aluminum ring at approximately 90 degrees. SR-4 type cement was used to hold the strain gauges because of its ability to bond to smooth surfaces. The strain gauges were wired in series and the wiring diagram is shown in Figure 4.

A slot 3/16 inch deep and 1-1/2 inches long was cut in each cylinder so that the aluminum rings could be placed around the cylinders. To hold the aluminum rings in place, two 4-1/2 inch diameter O-rings were placed in the slot on each cylinder. The aluminum rings were floated on the O-rings, and the remaining spaces between the cylinders and the edge of the aluminum rings were filled with rubber cement to absorb as much of the shock of driving as possible. A 1/4 inch diameter hole was drilled in each cylinder beneath each aluminum ring for the strain gauge wires. Figure 5 shows a typical load cell connection.

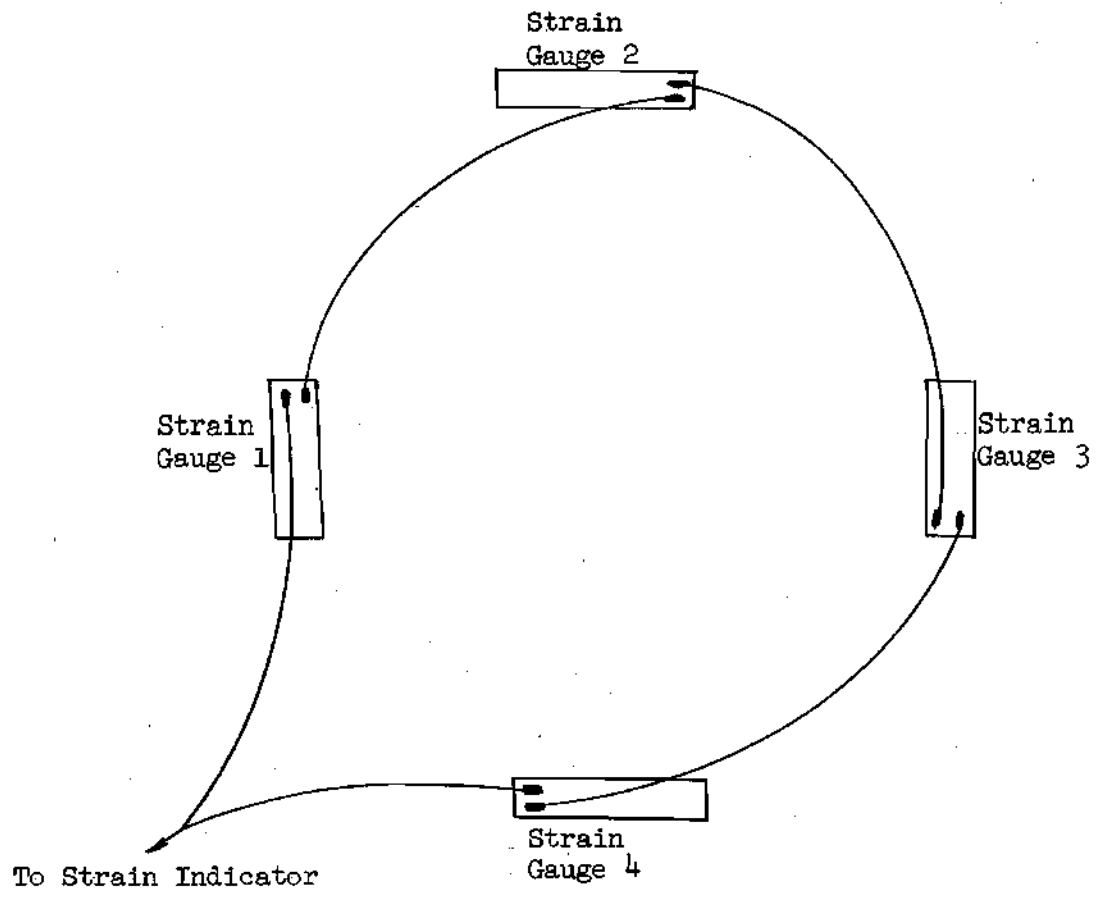


Figure 4. Wiring Diagram for Lateral Load Cells

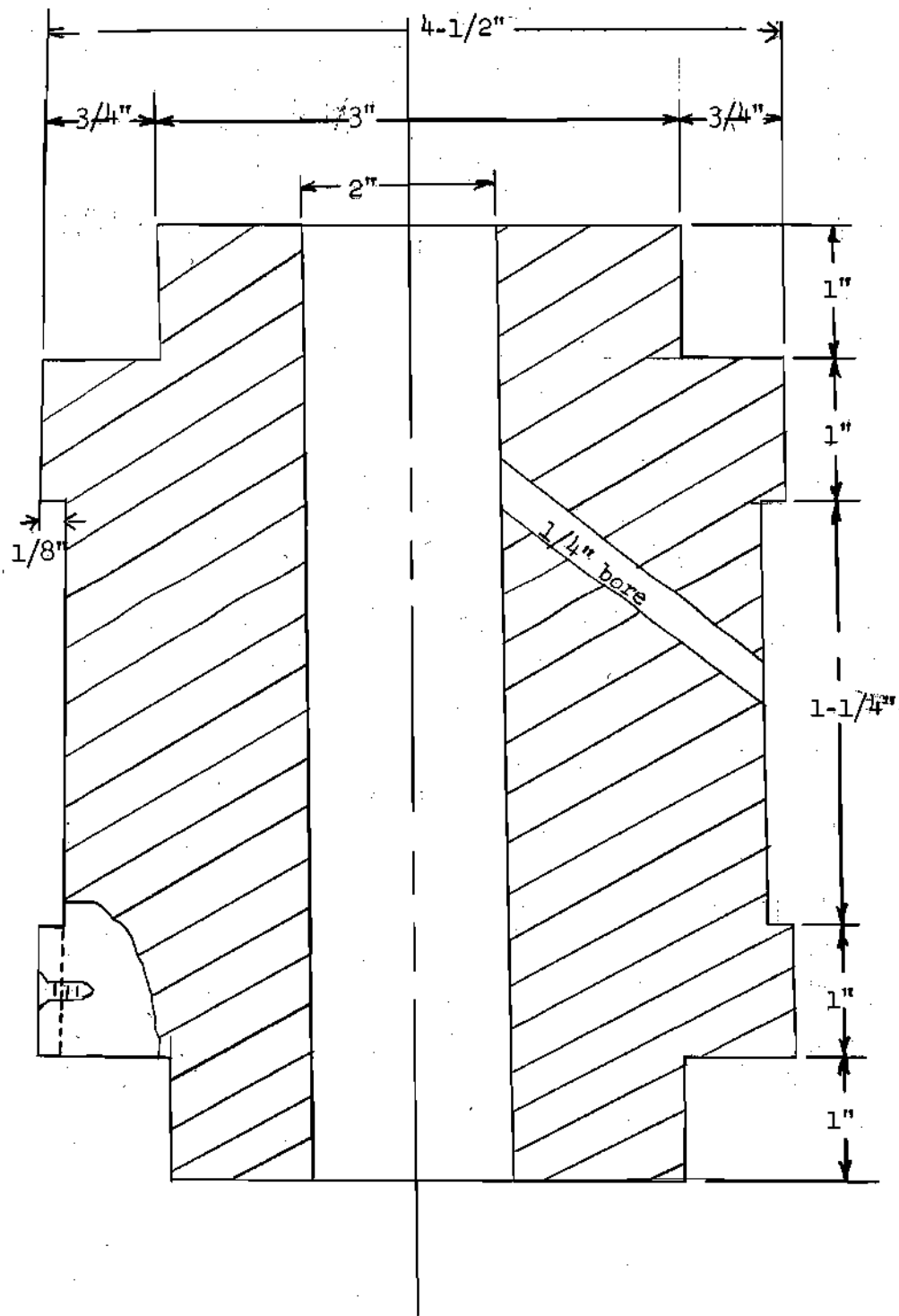


Figure 5. Lateral Pressure Load Cell

At the tip of the pile, a base plate was placed with devices for measuring both lateral and vertical pressures. The lateral pressure was measured by an aluminum ring placed by the same procedure used in the load cell connections. The maximum vertical pressure was calculated and a safety factor of four was used to design a proving ring for measuring the vertical pressures.

Since the dynamic force against the proving ring during driving was so much larger than the force applied against it during static loading, it was necessary to design an energy absorbing device. Two large screws $5/8$ inch in diameter were used to bear against the tip of the pile during driving and were released during testing. One-half inch diameter rods were placed from the top of the screws in the base plate to the top of the pile so that once the pile was driven the rods could be turned, thereby releasing the screws. Inside the proving ring, two SR-4 strain gauges were placed to measure the force on the base of the pile. Figure 6 shows a cross section of the base plate.

The test pit into which the pile was driven was eight feet and four inches in diameter and 22 feet deep. An A-frame provided a support for the pile driving equipment which consisted of leads, drop hammer, and a winch for lifting the hammer. A 200 ton capacity reaction frame and hydraulic jack were used for loading.

The soil used was obtained initially from the Chattahoochee River near Atlanta, and was a medium uniform sand composed mostly of sub-angular quartz particles but fairly rich in mica. Vesic (14) determined the maximum and minimum densities of the sand and the shear strength characteristics of the sand, and these are shown in Tables 2 and 3.

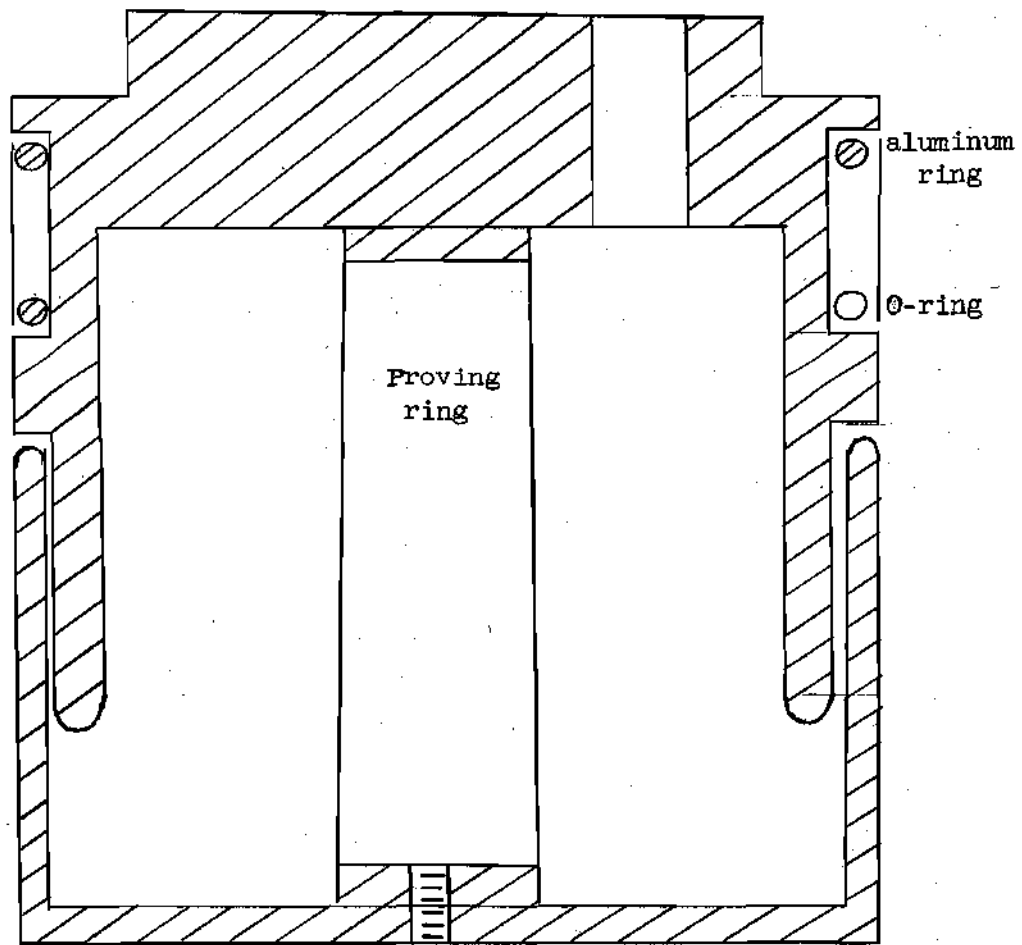


Figure 6. Base Plate Load Cell

Table 2. Maximum and Minimum Densities

Density	Dry Unit Weight lb/ft	Void e	Porosity n
minimum	79.0	1.10	52.4 %
minimum	102.5	0.615	38.1 %

Table 3. Shear Strength Characteristic

Angle on Internal Friction ϕ , degrees		Void Ratio e
$\sigma_3 < 10 \text{ lb/in}^2$	$10 < \sigma_3 < 80 \text{ lb/in}^2$	
----	44.3	.6
44.3	40.0	.7
40.5	36.2	.8
36.8	33.5	.9
34.0	31.0	1.0
31.9	----	1.10

Moving of the sand was done with a mechanical digger and conveyor belt. To ensure a relatively homogeneous mass, the test pit was filled by passing the sand through a number 10 sieve, eight feet in diameter. To check the homogeneity and density of the sand, a penetrometer coupled with a 12 foot long rod and a 3,000 pound air-hydraulic ram were used.

The ram could be raised or lowered by air forcing hydraulic oil into the jack. The jack was hung from a wide flange section above the test pit. The connection consisted of a steel frame three feet long that could rotate in a three foot radius about the pit so that tests could be run in different locations around the pit without disconnecting the jack. A proving ring was placed between the ram and the penetrometer rod. Calibration of the proving ring is shown in Figure 7. The penetrometer rod had a point diameter of $1/2$ inch and a shaft diameter of $3/8$ inch.

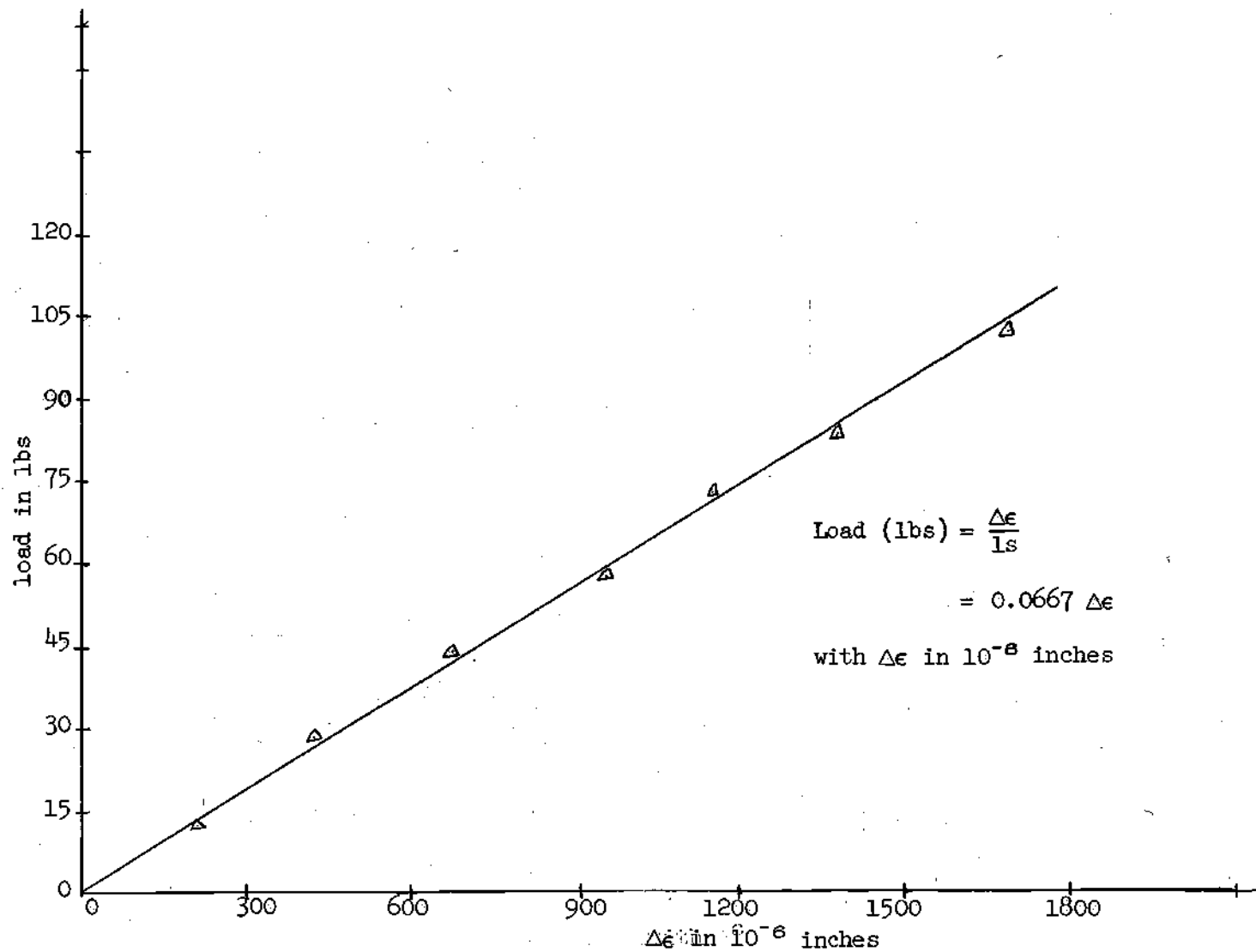


Figure 7. Penetrometer Proving Ring Calibration

CHAPTER IV

TEST PROCEDURE

Since no work had been done at Georgia Tech with a full scale pile instrumented to measure lateral earth pressures, it was necessary to design and construct the pile. A 4-1/2 inch outside diameter steel pipe with 3/4 inch walls was used as the shaft of the pile.

Both the lateral pressure against the side of the pile and the vertical pressure against its tip were desired. Once the lateral load cells were constructed, they were calibrated in a sand filled steel container, two feet in diameter by one foot in depth.

A load cell was placed in the sand, a rubber membrane and gasket were placed on the sand, and a steel lid was bolted to the container. The lid had an air pressure gauge and connection to enable the application of air pressure against the top of the sand. This air pressure represented a known surcharge, and readings on the cells were taken at various air pressures. The magnitude of these readings indicated the sensitivity of the load cells.

After each load cell had been checked out in the sand, it was calibrated under air pressure. First, each cell was sealed with rubber cement and wax and then placed in the same metal container as above without the sand. A plastic tube from the cell to the outside allowed the air inside the cell to remain at atmospheric pressure while the air pressure inside the container built up. Air pressures were measured with a Bourdon gauge,

and readings were taken at zero or atmospheric pressure and in increments of one psi until a value of 15 psi was reached. Figures 8, 9, 10, and 11 show the average curves of strains versus air pressures for each load cell. Each cell was tested five times to ensure that the results were consistent. The lateral pressure measuring ring on the base plate was calibrated in the same manner as the load cells.

The proving ring for measuring the vertical pressure against the tip of the pile was designed using the maximum calculated static load and a safety factor of four. The proving ring was loaded to approximately 10,000 pounds, a value equal to twice the anticipated maximum working load. The resulting calibration curve was linear, as shown in Figure 12.

The sand was removed from the test pit to a depth of approximately 18 feet with a mechanical digger and conveyor belt. The conveyor belt was rigged over the test pit to refill it. The eight foot diameter, 1.4 mm opening sieve was placed on the bottom of the pit resting on the sand surface. The sieve was first filled with sand falling from the conveyor belt, and then lifted so that the height of fall of the sand from the sieve was approximately 30 inches. This procedure was to ensure that there would be the same density in the pit from the bottom to the top.

Once the test pit was filled with sand, the pile driving equipment was placed in position. The leads or the hammer guides were hung from an A-frame located above the pit. The leads were placed over the center of the test pit, and the 500 pound hammer, consisting of lead weights bolted together, was placed in the leads and held there by an anchored winch located on the floor adjacent to the pit.

After the sand was placed and the pile driving equipment was set up,

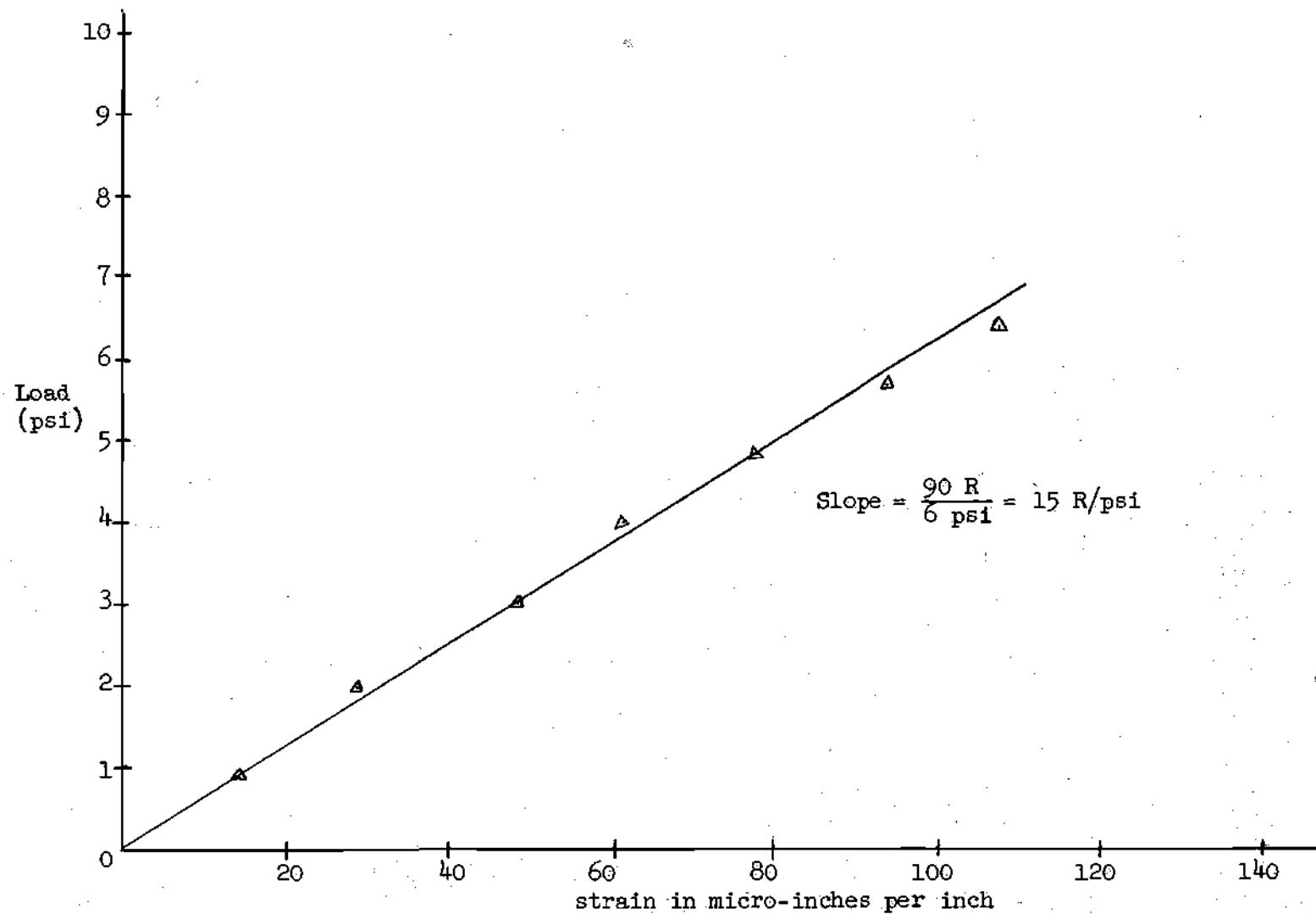


Figure 8. Gauge 1 -- Lateral Load Cell Calibration

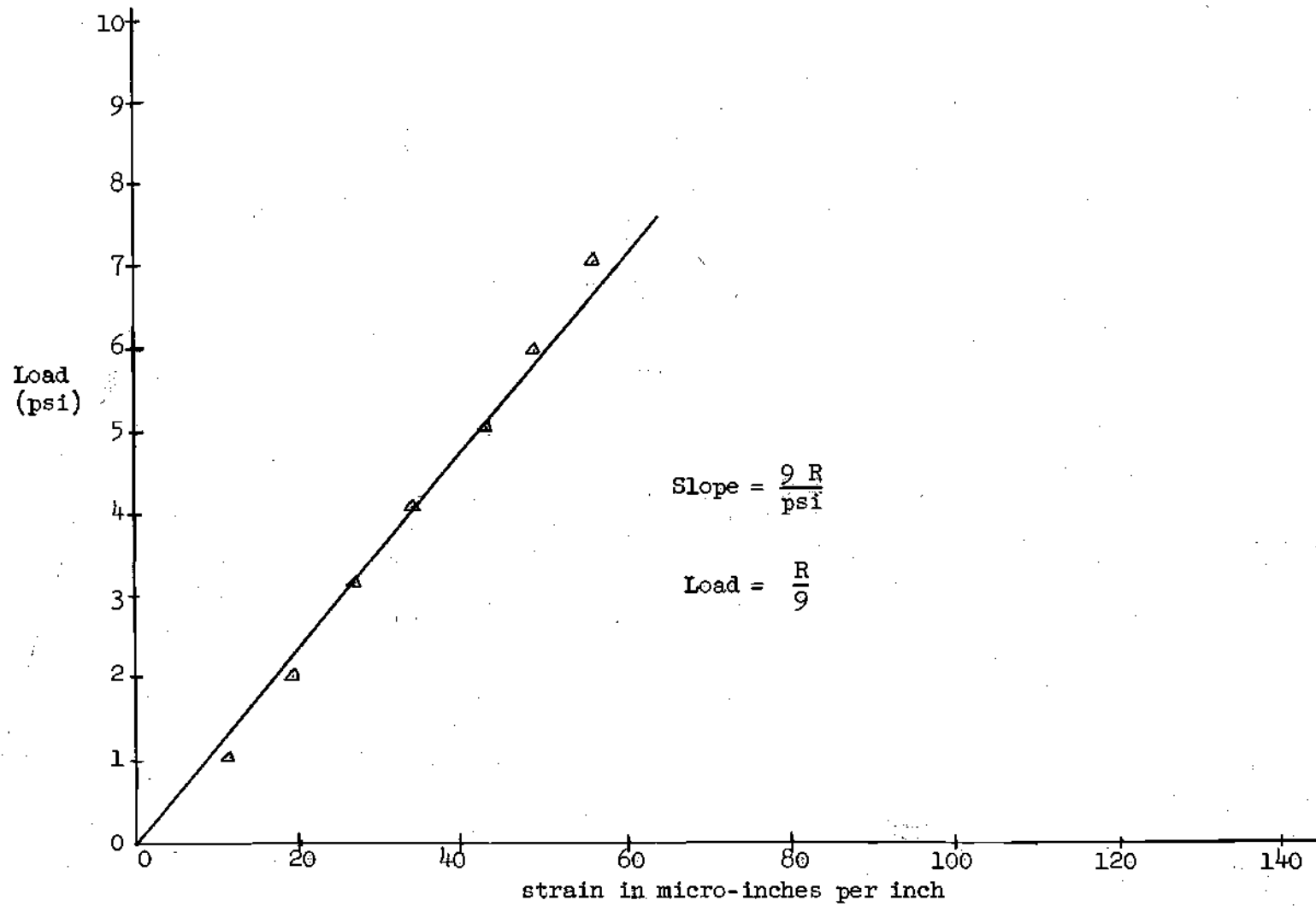


Figure 9. Gauge 2 -- Lateral Load Cell Calibration

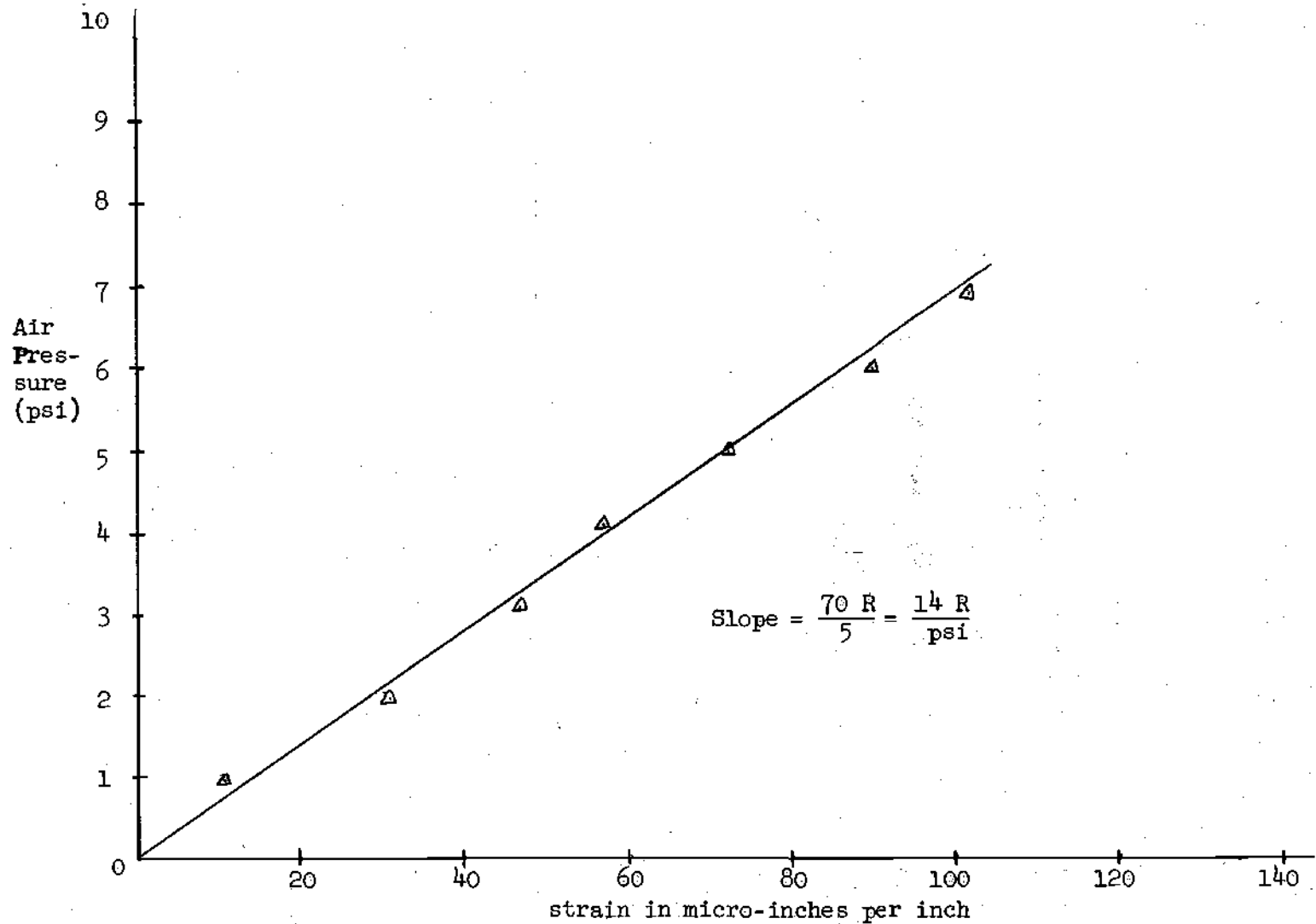


Figure 10. Gauge 3 -- Lateral Load Cell Calibration

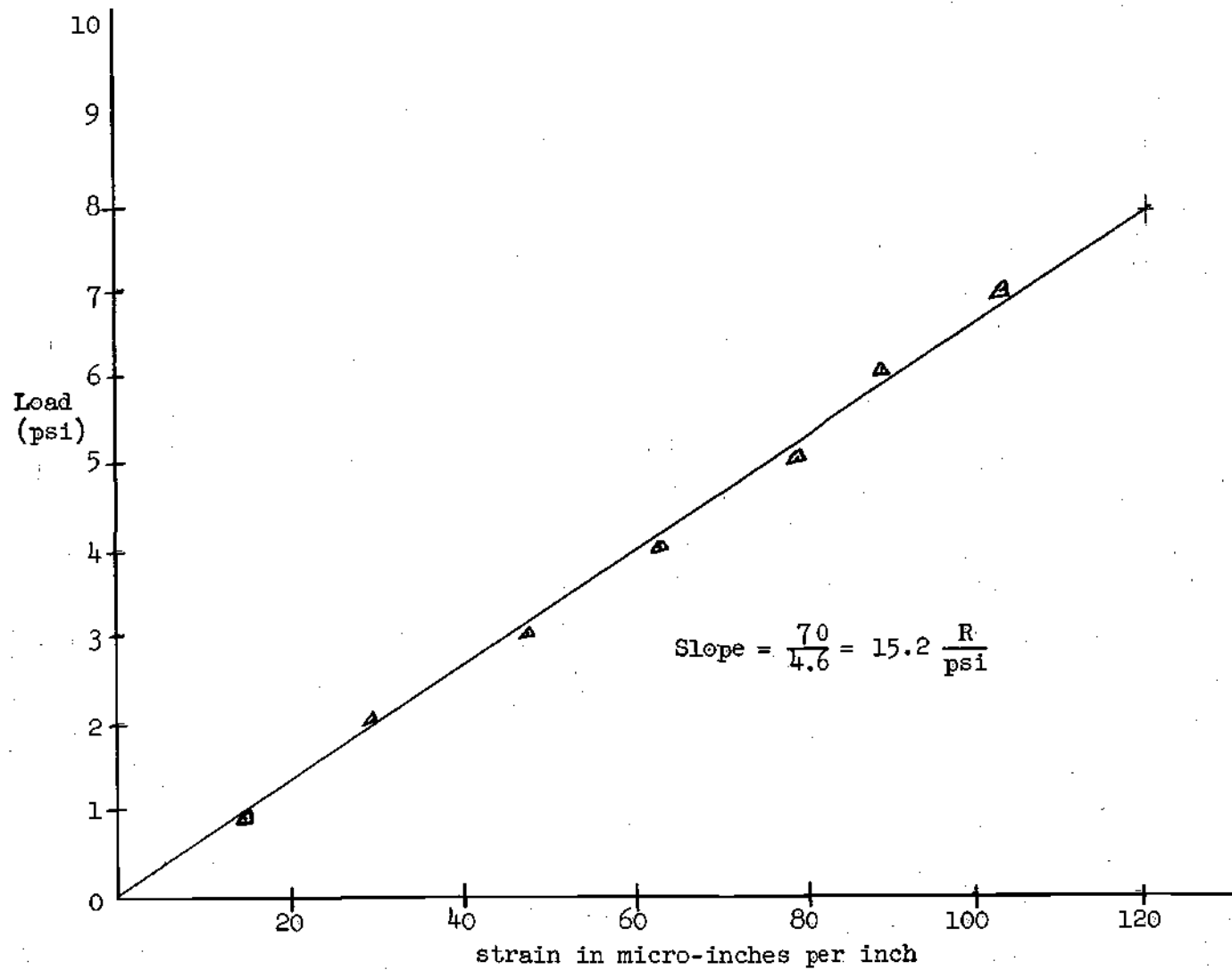


Figure 11. Gauge 4 -- Lateral Load Cell Calibration

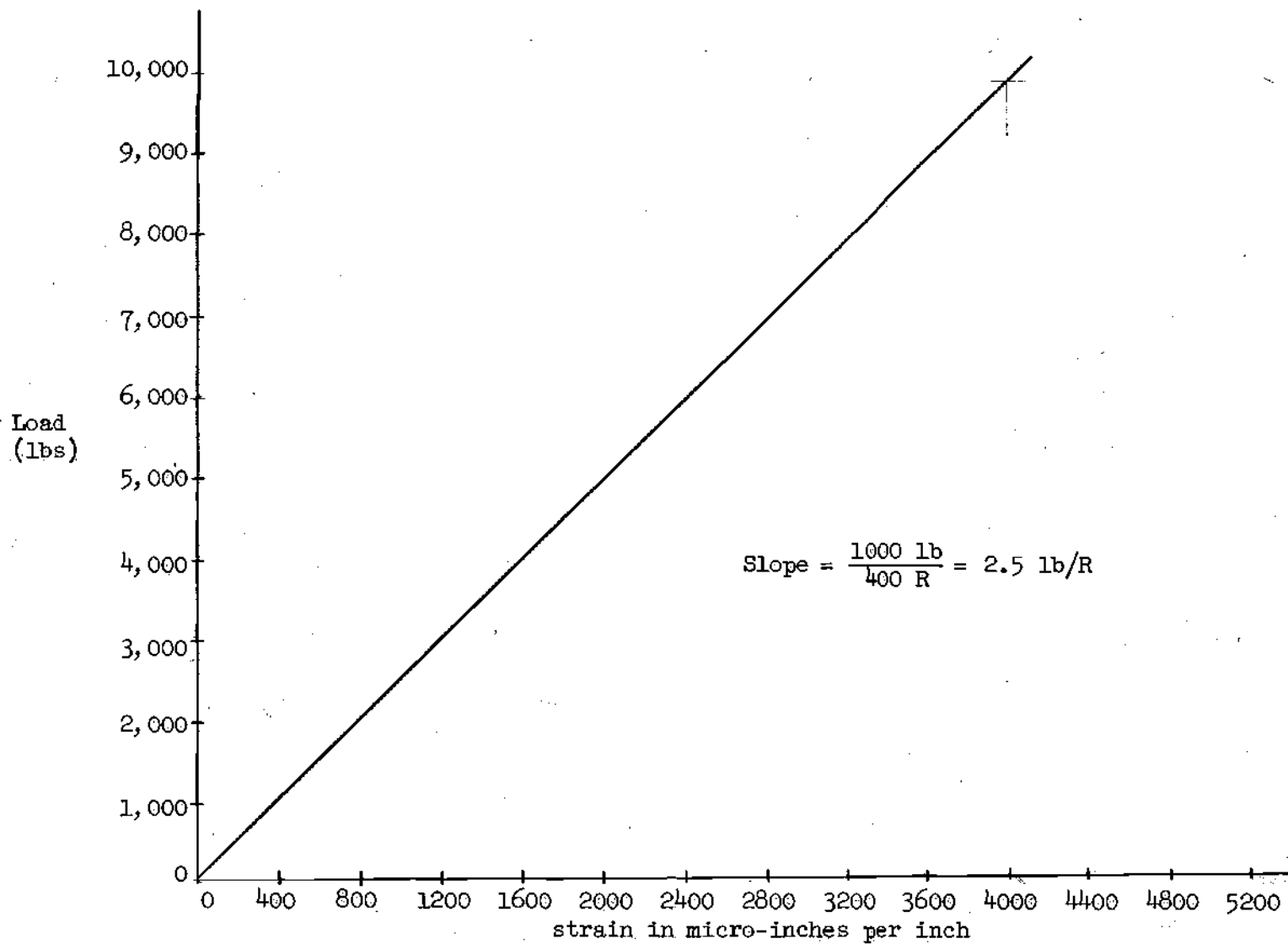


Figure 12. Base Plate Proving Ring Calibration

the first 10 feet of the pile was brought to the test pit for driving. The pile was held in place under the hammer by collars at the top and bottom of the pile. Driving was done by lifting the hammer with the winch and allowing it to drop freely.

During the first driving, the connection between the screw jack and the rods broke and no vertical pressure readings could be taken. Readings were taken from the lateral pressure measuring load cells, and the ultimate bearing capacity of the pile was determined by loading and failing the pile. After redesign, a satisfactory connection between the rods and screw jacks was developed. This connection allowed the rods to move up and down during driving.

Once this new design was constructed, the pile was driven again, and both lateral and vertical pressure readings were taken. Readings were taken before driving and after driving. The pile was loaded to failure, and readings were taken during failure.

Loading of the pile was done by swinging the leads to one side and moving a large steel frame and ram over the pile. The frame was bolted to the floor, and the ram was bolted to the frame. The ultimate bearing capacity of the pile was determined by jacking down on the pile and reading the maximum load on the gauge.

Uniformity and density of the sand in the test pit was checked by penetrometer tests after the pile was removed. The leads and hammer were pulled to one side, and the 1,000 pound movable crane was moved over the pit. A swivel steel frame with a three foot radius was connected to the beam and the 12 foot long, 3,000 pound capacity air-hydraulic jack was connected to it.

A proving ring placed between the ram of the jack and the penetrometer rod allowed readings to be taken as the rod was pushed into the sand. The total resistance to penetration of the rod at four different locations around the test pit was taken. The density of the sand was estimated from Vesic's calibration curves (15) relating penetration resistance to density, as depicted in Figure 13.

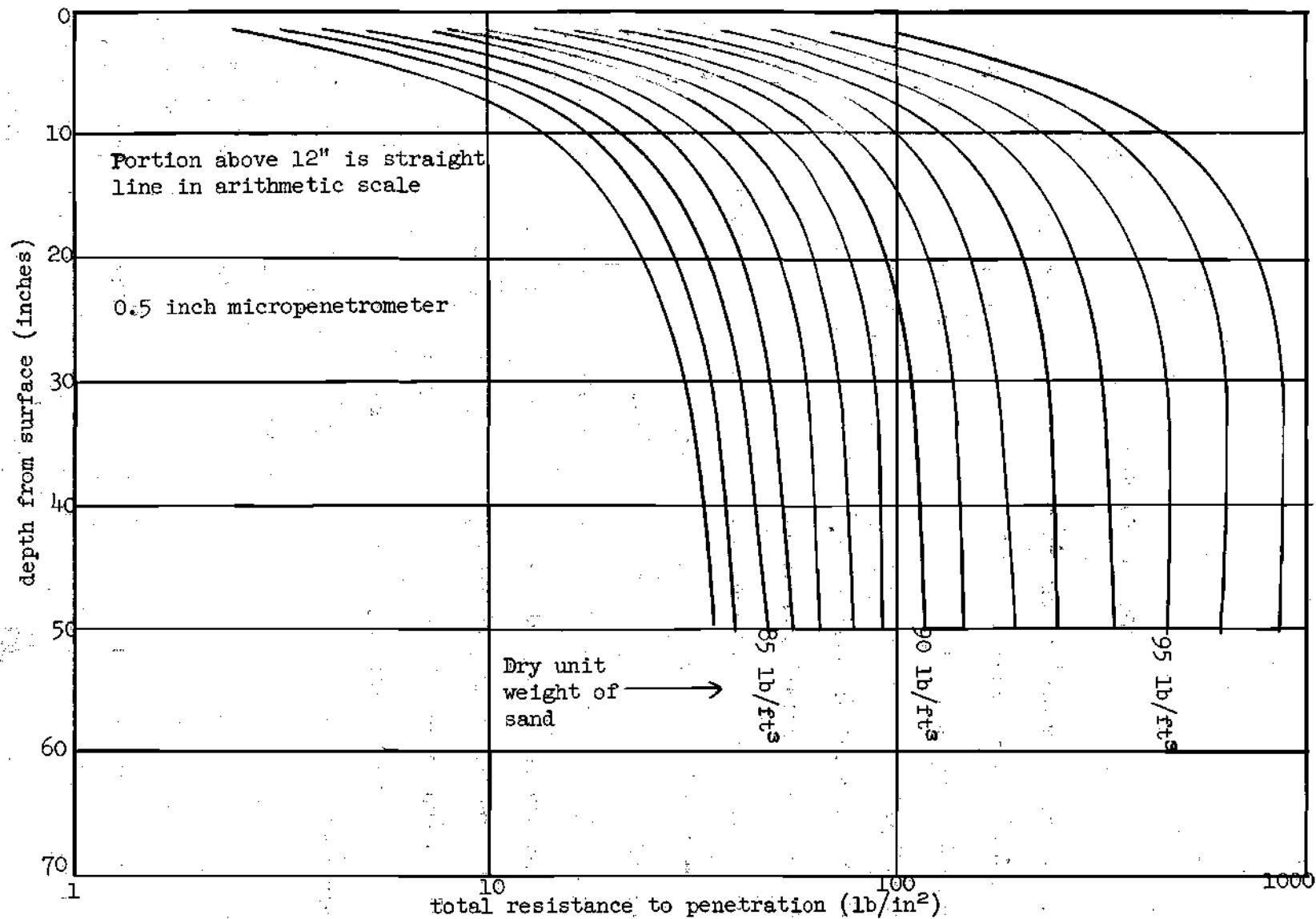


Figure 13. Relationship Between Depth and Total Penetration Resistance for Different Sand Densities

CHAPTER V

DISCUSSION OF RESULTS

The purpose of this investigation was to determine the lateral and vertical pressures acting on a pile driven into a cohesionless soil to better determine the ultimate bearing capacity of a pile. A pile was designed, constructed, driven, and loaded to failure to accomplish this.

The average penetrometer results are shown in Table 4. Vesic (16) plotted curves of penetrometer resistances at different depths versus the density of the sand. Vesic's curves were determined by sounding sand models in a 24 by 16 by 60 inch box placed on a scale and filled with sand by the same procedure used when filling the pit. Because of the shallow depth of the models, Vesic's curves may not be valid at greater depths.

Comparison of penetrometer results with Vesic's curves showed the unit weight of the sand to be approximately 84 pounds per cubic foot. Since the sand was placed by a gravity fall of 30 inches through a 1.4 mm sieve, it was not expected to have a high relative density. The minimum density of this sand was 79 pounds per cubic foot, and the maximum density was 102 pounds per cubic foot.

Vesic, in his paper to the Highway Research Board (17), expressed e , the void ratio of the sand, as a function of ϕ , the angle of internal friction of the sand. He did this by running triaxial shear tests on 54 air-dry samples 2.8 inches in diameter and approximately six inches high. Assuming the Mohr-Coulomb criterion of failure to be valid, Vesic derived

Table 4. Penetrometer Test Results

Depth (in)	Load (lbs)
10	35
20	30
30	35
40	37
50	40

$$\gamma \approx 84 \text{ lb/ft}^3$$

In place density tests at surface

Test	Density
1	85.4 lb/ft ³
2	84.3 lb/ft ³
3	85.1 lb/ft ³

the following expression which is valid when the confining pressure is less than 10 pounds per square inch.

$$\tan \phi = \frac{.68}{e} \quad (14)$$

Using this expression, ϕ for this test was determined to be approximately 34 degrees. These values for density and angle of internal friction were used in the calculations of the bearing capacity of the pile.

Two pile loading tests were conducted in this program. In the first test the pile was driven a depth of 10 feet and in the next test the pile was driven 15 feet. For both tests, readings were taken on all gauges before driving and after the pile had reached the desired depth. The difference in these readings represented the lateral pressures against the pile at various depths and the vertical pressure against its tip. The pile was loaded until failure and readings were taken.

Pile Depth of 10 Feet

At 10 feet, the force the sand exerted on the tip of the pile was 1,590 pounds. The maximum load the pile could take before failure was determined by loading the top of the pile until the pile began to fail and could take no more load. This load was 4,700 pounds.

The area of the base tip was determined to be 0.11 square foot. Using the bearing-capacity factors for deep cylindrical foundations adapted from Meyerhof (17) in the general bearing capacity equation, the maximum base force was calculated to be 5,980 pounds. This is higher than the value actually measured against the base of the pile. The steepness of

the bearing capacity factors, angles of internal-friction curves, could account for this. A slight error in the magnitude of ϕ would cause a large difference in load. Meyerhof's factors may be somewhat larger than that actually reached in the sand and, hence, on the unsafe side.

The actual maximum load on the base plate was subtracted from the maximum total bearing capacity taken from the gauge on the jack and was 4,336 pounds. This value was assumed to be taken by side friction.

The value of side friction was calculated using an average K of 0.5 and an angle of friction of 34° and was found to be 1,736 pounds. This value is 2,610 pounds less than the load attributed to the side load. Since the overburden pressure at a certain depth can be calculated with reasonable accuracy, it is reasonable to assume that the average value of K must be greater than 0.5.

Using a triangular pressure distribution in which the lateral pressure at ground surface was zero and increased linearly until the maximum pressure was reached at the base of the pile, the average value of K necessary to create the calculated side friction can be computed. This value was equal to approximately 1.2. This means that, due to driving and volume displacement, the sand around the pile was densified, which increased the lateral pressure against the pile. Sowers and Sowers (18) state that the value of K for a pile driven into a loose cohesionless material is approximately one. This agrees closely with the results obtained here.

The results of the lateral pressure load cells are shown in Table 5.

Table 5. K versus Pressure and Depth

Depth (ft)	Measured Pressure (psi)	Calculated K's from Pressures
4	4.5	1.8
8.5	5.1	1
10	6	1

The above table indicates that K was larger near the top of the pile and gradually decreased as depth along the pile was increased. The actual and triangular pressure distribution curves are shown in Figure 14. The actual pressure against the side of the pile is seen to increase rapidly at first but more slowly with increasing depth.

The area under the actual pressure distribution curve was calculated and compared with the area under the triangular pressure distribution curve. The two areas were approximately equal which indicates that the assumption of a triangular pressure distribution will give good results in finding the load carrying capacity of a pile, if average K is used.

Pile Depth of 15 Feet

At a depth of approximately 15 feet, the maximum failure load was 13,460 pounds. Because of the large ram area and small gauge readings from the jack, there was a possibility of error in the range of 10 percent. The calculated base load using the general bearing capacity equation with Meyerhof's bearing capacity factors was larger than the actual load indicated by the base plate proving ring. The actual base load was 6,246

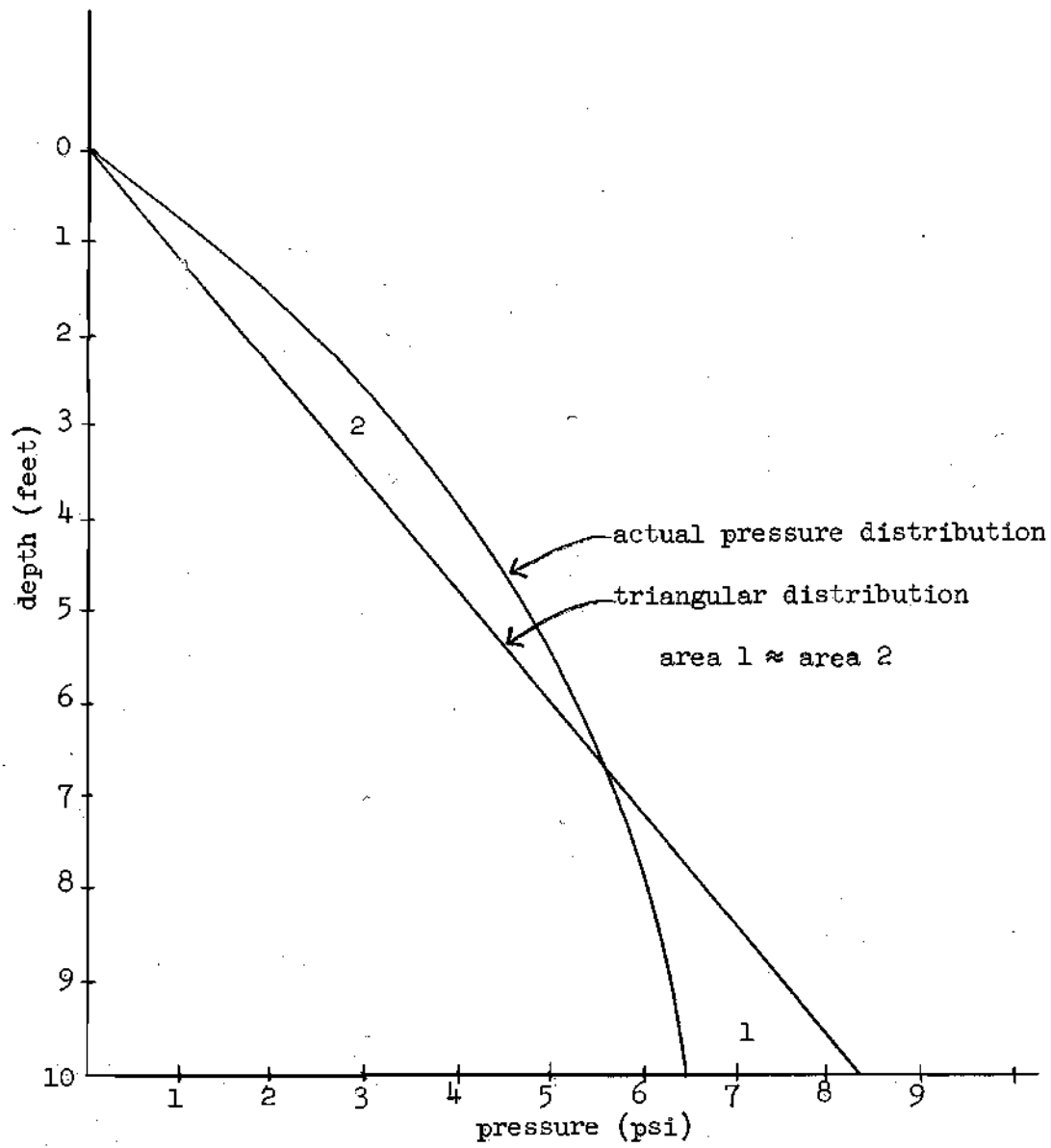


Figure 14. Area Pressure Curves at 10 Feet

pounds, and the calculated load was 9,100 pounds.

The measured load against the tip of the pile was subtracted from the failure load and was 7,214 pounds. This value was assumed to be taken by side friction. Using a triangular pressure distribution, the average value of K necessary to produce this load was 0.925. This was lower than the K for the 10 foot section. There could possibly be an error in one or more of the readings, or it could mean that the average value of K decreases with pile depth.

The lateral pressures against the side gauges for the same depth as in the 10 foot section were somewhat lower, as shown below in Table 6.

Table 6. K versus Pressure and Depth

Depth (ft)	Measured Pressure (psi)	Calculated K's from Pressures
4	3.5	1.5
8.5	4.9	1
13	5.7	.72
14.5	5.9	.7

Figure 15 shows the measured pressure against the side of the pile for a depth of 15 feet. On the same figure, a triangular pressure distribution curve is drawn using the calculated value of K. The two areas are approximately equal.

During failure of the pile, the strain indicator for the lateral

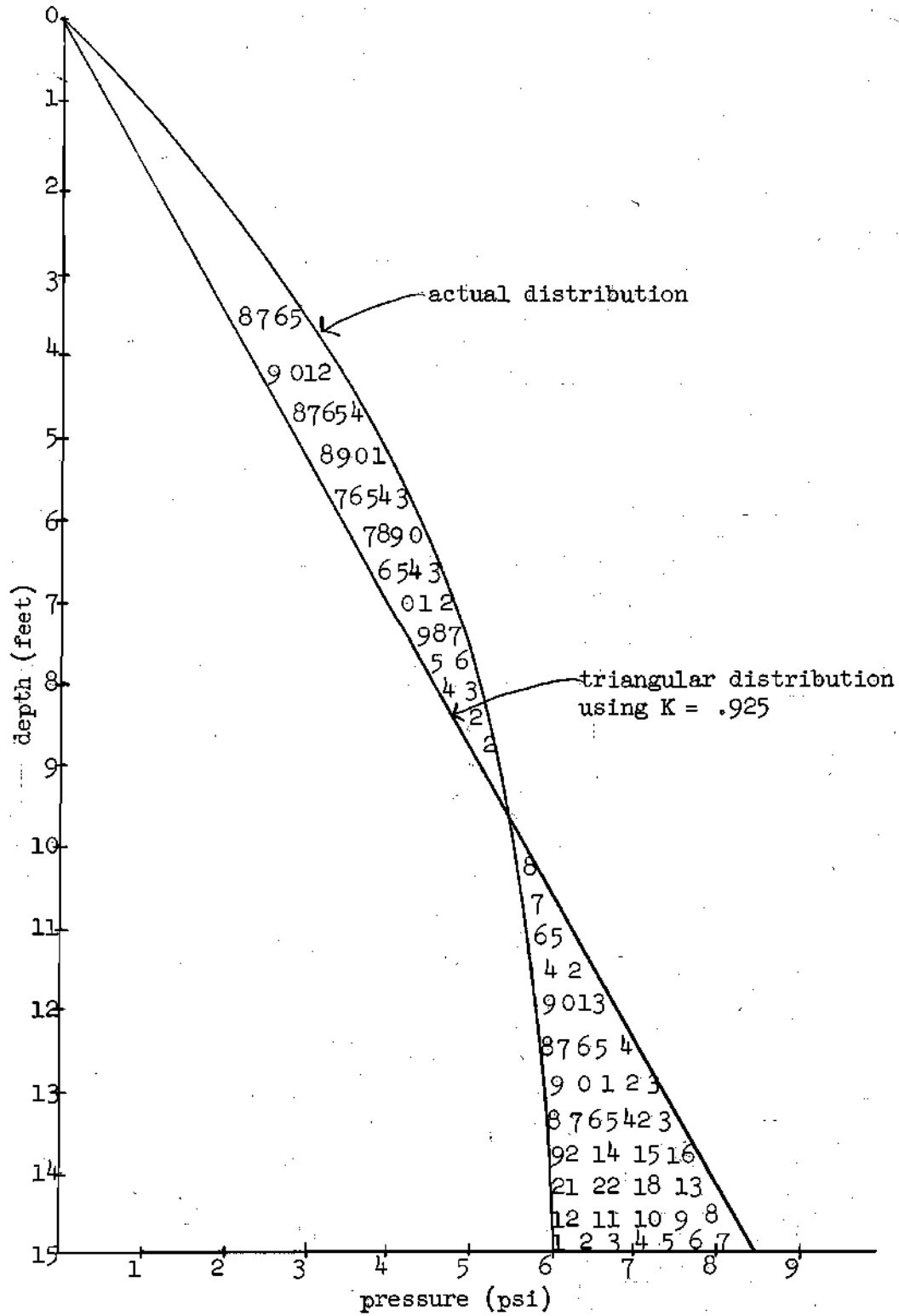


Figure 15. Area Pressure Curves at 15 Feet

lateral pressure gauges was left on to see what happened to the lateral pressure against the pile. As the pile was pushed into the sand, the indicator showed a slight drop off of lateral pressure.

CHAPTER VI

CONCLUSIONS

The following conclusions apply to a pile driven in the Chattahoochee River sand which was used.

1. The lateral pressure coefficient, K , is a maximum near the top of a pile and it decreases with depth.

2. The average value of K decreases with an increase in the length of a pile.

3. Using a triangular pressure distribution curve, the value of K necessary to produce the measured skin friction load was approximately one.

4. A triangular pressure distribution is a good approximation in determining the bearing capacity of a pile, using an average K .

5. The lateral pressures decrease slightly as the pile is failed and pushed into the ground.

6. The general bearing capacity equation using Meyerhof's constants gives values approximately 25 percent larger than those measured.

CHAPTER VII

RECOMMENDATIONS

1. Greater effort should be used to achieve a uniform sand, and a more accurate method of obtaining the density of the sand should be determined.

2. Since lateral pressure distribution is so important in the calculations of the bearing capacity of a pile, further investigation should be directed to this end, using both full scale and model piles.

BIBLIOGRAPHY

1. Hansen, B., "Simple Statistical Computation of Permissible Pile Loads," Christiani and Nielsen Post, No. 13, 1951.
2. Terzaghi, Karl, Theoretical Soil Mechanics, 1st ed., New York: John Wiley and Sons, Inc., 1943.
3. Caquot, M., "Equilibre des Massifs Pulverulents a Frottement Interne," Gauthier-Villiers, Paris, 1934.
4. Skempton, A. W. and A. A. Yassin, "Theorie de la force portante des pieux dan le sable," Annales de l'Institut Technique du Bati-ment et des Travaux Publics, 1952.
5. Meyerhof, G. G., "The Ultimate Bearing Capacity of Wedge-shaped Foundations," Proceedings, 5th International Conference on Soil Mechanics and Foundations Engineering, Paris, 1961.
6. Terzaghi, Karl, Theoretical Soil Mechanics, 1st ed., New York: John Wiley and Sons, Inc., 1943.
7. Norlund, R. L., "Bearing Capacity of Piles in Cohesionless Soils," Journal of Soil Mechanics, Vol. 89, No. SM3, May 1963, p. 1.
8. Caquot, A. and J. Kerisel, "Tables for the Calculation of Passive Pressure, Active Pressure and Bearing Capacity of Foundations," Gauthier-Villiers, Paris, 1948.
9. Terzaghi, Karl, as quoted by B. Broms, "Discussion on Bearing Capacity of Piles in Cohesionless Soils," Journal of Soil Mechanics, Vol. 89, No. SM6, Nov., 1963, p. 5.
10. Broms, B., "Discussion on Bearing Capacity of Piles in Cohesionless Soils," Journal of Soil Mechanics, Vol. 89, No. SM6, Nov., 1963.
11. Kezdi, A., "Bemerkungen zur Frage der Tragfahigkeit von Pfahlgrup-pen," Symposium on Pile Foundations, Stockholm, Sweden, 1960, pp. 89-96.
12. Silberman, J. O., "Some Factors Affecting the Frictional Resistance of Piles Driven in Cohesionless Soils," Thesis presented to Cor-nell University, Ithaca, N. Y., June 1961.
13. Sowers, G. B. and G. F. Sowers, Introductory Soil Mechanics and Foundations, The MacMillan Company, New York, 1961, p. 207.

BIBLIOGRAPHY (Concluded)

14. Vesic, A. B., "Bearing Capacity of Deep Foundations in Sand," Annual Meeting of Highway Research Board, Washington, D. C., Jan. 7-11, 1963.
15. Ibid., Table 2.
16. Ibid., Figure 13.
17. Ibid., p. 11.